144 Turbulence Anisotropy in an Urban Canyon and Intersections
(Formerly P2.1)

Cheryl Klipp, PhD *
US Army Research Lab, Adelphi, MD
16th Conference on Air Pollution Meteorology

1. Abstract

Turbulence near a solid surface is not isotropic, since motions perpendicular to the surface are limited by the presence of the surface. As a consequence, the turbulent variance, and therefore dispersion, is greater in some directions than in others at any location in an urban boundary layer. A better characterization of the anisotropy should lead to better modeling of turbulent dispersion in complex environments.

Using data from JU2003, the degree of anisotropy as well as the largest and smallest dispersion directions will be shown for various locations in the Park Avenue canyon as well as at the intersections at either end of the canyon. Values for an open area will also be shown for comparison.

2. Data

For this analysis, data from the Joint Urban 2003 field campaign Park Avenue street canyon of Oklahoma City, OK are used from days 182-196, Jul 1-15, 2003 (Fig. 1).

The intersection SPWIDS packages include RM Young 81000 3D sonic anemometers mounted about 8 m above street level. The OU profile tower, about 8m from the south side of the canyon, has 5 RM Young 81000 sonics. Only the ones at 1.5m and 15.7m are used here. The rooftop overhang sonic is 47.5m above ground level (agl), 1.75m away from the side of the building and about 0.3 m below the building wall top. The other rooftop sonic is mounted on a flagpole 3.7m above the roof, 47.7m agl. Both are Metek USA-1 3D sonics (Brown *et al* 2003).

Also used are 2D wind data (PWIDS) from the post office roof, about 25m above a 5 story building about 0.6 Km SSW of the Park Avenue canyon.

Open area data are from the Army Research Laboratory's tower at the transit center bus parking lot about 6 KM SW of downtown. The RM Young 81000 sonic anemometer is 10m agl.

* Cheryl Klipp, ARL, RDRL-CIE-D, 2800 Powder Mill Rd, Adelphi MD 20783, 301-394-2543, cheryl.l.klipp@us.army.mil

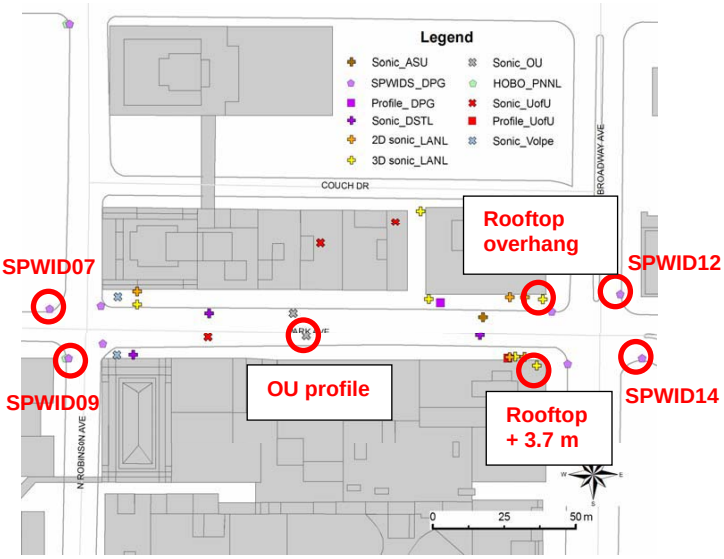

Map from Allwine and Flaherty 2006: PNNL-15967

Figure 1: Locations of instruments used in this analysis. Map is of one block of Park Avenue in Oklahoma City.

3. Reynolds Stress Tensor

For each sonic anemometer, the variances and covariances were calculated using 15 minute non-overlapping blocks of data. The resulting six values make up the Reynolds stress tensor, a 3x3 real symmetric (Hermitian) matrix. The eigenvalues, λ_i, of this matrix are the fundamental turbulent variances, each associated with the direction of the corresponding eigenvector, Λ_i (Arfken 1985).

Over open terrain for neutral stratification, the eigenvectors are nearly aligned with the streamwise, cross-stream, vertical coordinate directions, differing by a 17° rotation about the cross-stream axis (Klipp 2007). The orientations of the eigenvectors in the Park Avenue canyon vary according to location in the canyon as well as by the incident wind direction as measured at the post office building 0.5 Km south of the central business district.

4. The Barycentric Anisotropy Map

The eigenvalues of the Reynolds stress tensor form the basis of the barycentric map of turbulence anisotropy (Banerjee *et al.* 2007). Perfectly isotropic turbulence, $\lambda_B = \lambda_M = \lambda_S$, will map at the C_3 vertex at the top of the triangle. Turbulence with $\lambda_B = \lambda_M$ and $\lambda_S = 0$ will plot at the bottom left vertex, C_2. Turbulence with $\lambda_B > 0$ and $\lambda_M = \lambda_S = 0$ will plot at the bottom right vertex, C_1.

If $\lambda_B = \lambda_M > \lambda_S$, the turbulence will plot along the left side: pancake-like turbulence. If $\lambda_B > \lambda_M = \lambda_S$, the turbulence will plot along the right side: cigar-like turbulence.

5. Open Area Results

As plotted on the barycentric map, the open area turbulence (Fig. 2) is not isotropic (at the C_3 point), nor does it have one or two vanishing eigenvalues (at the bottom line). It is not cigar-like, having one larger eigenvalue and two similar, nearly equal eigenvalues (the right hand line). Sometimes the anisotropy is pancake-like in that there are two larger, similar eigenvalues and one smaller value. For the most part, the open area anisotropy falls between these extremes.

The directions of the eigenvectors associated with the largest and smallest eigenvalues (Table 1) are related to the streamwise, cross-steam and vertical coordinates by a rotation of 17° around the cross-stream axis consistent with wind tunnel studies (Hanjalic and Launder 1972).

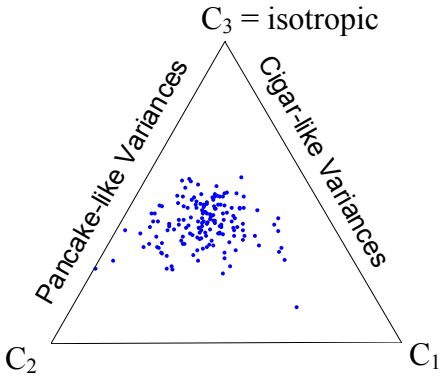

Figure 2: Barycentric plot of open area turbulence anisotropy.

Table 1: Average direction of eigenvectors associated with largest and smallest eigenvalues for open area turbulence for all reference wind directions 135° and 225° at post office.

	Eigen vector	Average Direction of Eigenvector
10m	Λ_S (small)	17° from vertical toward the mean wind direction (standard deviation 5 °)
	Λ_B (large)	17° below horizontal toward mean wind direction (standard deviation 7 °)

6. Wind Drection Dependence

During this 15 day period, winds were primarily out of the south, with about 90% of all mean wind headings between 135° and 225° (Fig. 3). For this paper, mean winds from 135° – 165° will be referred to as SE, 165° – 195° as S, and 196° – 225° as SW.

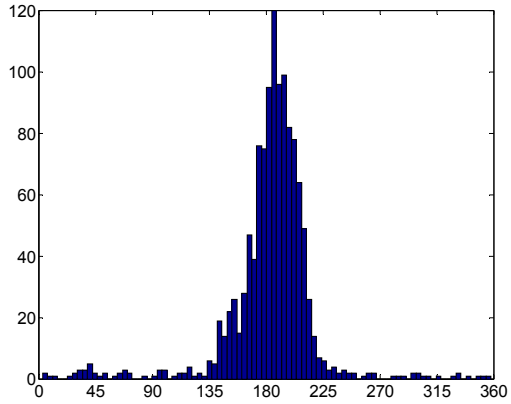

Figure 3: Distribution of mean wind directions for days 182-196 as measured at the post office south of downtown.

7. Results

Information about the type of anisotropy and tables of eigenvector directions are given in figures 4 – 9 for two levels of the OU tower and two LANL rooftop locations. The information is separated into the three wind categories given above.

Of the two OU tower levels, the 1.5m shows the most variation in anisotropy type (figures 4-6), from close to pancake shaped for SW winds to close to cigar shaped for SE winds. The large and small eigenvector directions are fairly similar for

the SE and S wind conditions compared to the eigenvector directions for SW winds. This may be in part to the fairly small number of samples of SE data.

The 15.7m level anisotropy is more cigar-shaped for all incident wind directions. This indicates similar degrees of restricted motion in two directions, presumably the street and the building wall. The eigenvector associated with the large eigenvalue, however, points in a direction roughly perpendicular to the canyon wall rather than parallel to it, in contradiction to the theory that the wall should be restricting turbulent motion. This could be a phenomenon related to wind tunnel anisotropy studies where eddy shape and turbulent variances are inversely related. In the process of squeezing the eddies along one axis, the variances in that direction are enhanced (Choi and Lumley 2001).

The turbulence above the canyon (figures 7-9) is closer to isotropic than the turbulence inside the canyon. The location overhanging the canyon at about building height is also closer to isotropy than at locations over open terrain. This could be a common feature of the enhanced turbulence found at building height over urban canyons (Roth 2000). Also the eigenvector directions are more scattered for this location and the average direction is very different compared to the other locations. This may be a measurement limitation, since as the turbulence approaches isotropy, all directions become similar making it difficult to get precise eigenvector direction calculations. It may also be a real effect of this enhanced turbulence zone. Further study will be needed.

The shift in anisotropy shape and eigenvector directions for the rooftop location are possibly in response to the complex structure on that building top, most notably the influence of structures to the west of the sonic, the tops of which are higher than the sonic elevation.

Preliminary findings for the intersections are shown in figures 10-13. These show the isotropy maps for all wind directions (from 135°-225°) for a single location on a single plot with marker color indicating wind direction. The SPWID07 location has the most notable incident wind direction dependence (fig 10), with SE winds being noticeably less cigar shaped than the other wind directions. SPWIDS 09 and 14 (figures 11 and 13) also have cigar-like variances with only subtle differences due to incident wind direction. The turbulence at SPWID 12 (fig 12) is less cigar-like than the other intersection locations, and for some cases, is nearly as isotropic as the roof overhang location. Eigenvector direction analyses have yet to be done for the intersections.

For the intersections and OU tower location, street trees may have an influence on the isotropy of the turbulence. This possibly important influence has not yet been investigated.

8. Conclusions

Anisotropy of the turbulence differs in urban canyons compared to open areas. These differences are important for dispersion in urban areas since many dispersion models were developed based on data from open areas. As more is learned about these differences, computer models of urban pollutant dispersion will be improved. More needs to be learned about the effects of stability on the anisotropy for both open areas and urban areas.

Street trees are expected to be an important factor in the degree and nature of the anisotropy in the canyon and intersections. How far this influence propagates is not known and is a subject of future research.

References

Arfken, G., 1985: *Mathematical Methods for Physicists*, 3rd ed., Academic Press, New York, 985 pp.

Banerjee, S., R. Krahl, F. Durst and Ch. Zenger, 2007: "Presentation of anisotropy properties of turbulence, invariants versus eigenvalue approaches." *Journal of Turbulence*, **8**, DOI: 10.1080/14685240701506896

Brown, M., D. Boswell, G. Streit, M. Nelson, T. McPherson, T. Hilton, E. R. Pardyjak, S. Pol, P. Ramamurthy, B. Hansen, P. Kastner-Klein, J. Clark, A. Moore, D. Walker, N. Felton, D. Strickland, D. Brook, M. Princevac, D. Zajic, R. Wayson, J. MacDonald, G. Fleming, D. Storwold, 2003: "Joint URBAN 2003 Street Canyon Experiment". AMS Conf. on Urban Zone, Seattle, WA, LA-UR-03-8454, 12 pp

Choi and Lumley, 2001: *Journal of Fluid Mechanics*, **436**, 59-84.

Hanjalic, K., and B. E. Launder, 1972: "Fully developed asymmetric flow in a plane channel." *J. Fluid Mech.*, **51**, 301 – 335.

Klipp, C. L., 2007: "A coordinate system independent surface stress". 7th Symposium on the Urban Environment, San Diego, CA.

Roth, M., 2000: "Review of atmospheric turbulence over cities." *QJR Meteorol. Soc.* **126**, 941 – 990.

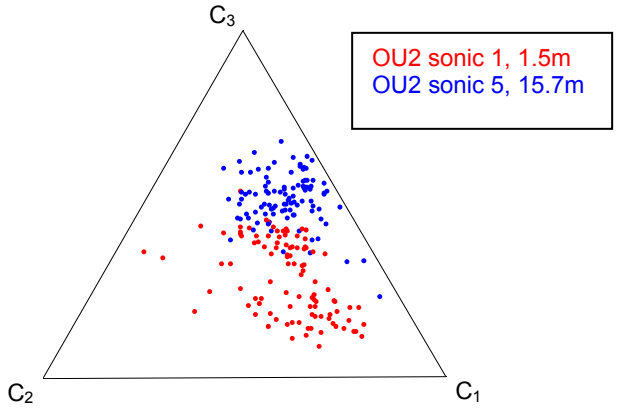

SE PO winds	Eigen vector	Average Direction of Eigenvector
1.5m	Λ_S (small)	11° from vertical toward the SE, 138°
	Λ_B (large)	9° above horizontal toward the NW, 323°
15.7m	Λ_S	35° from vertical toward the W, 276°
	Λ_B	1.7° above horizontal toward the N, 15°

Figure 4: Anisotropy map of two locations on OU2 tower for SE post office winds and table of directions for average eigenvectors.

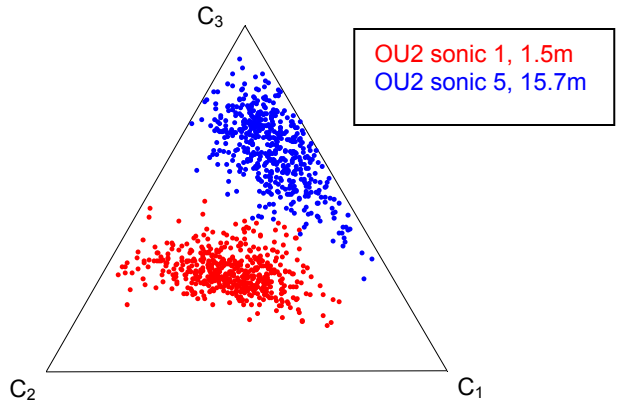

S PO winds	Eigen vector	Average Direction of Eigenvector
1.5m	Λ_S (small)	7° from vertical toward the SSE, 157°
	Λ_B (large)	5° above horizontal toward the NW, 320°
15.7m	Λ_S	35° from vertical toward the W, 277°
	Λ_B	1.3° above horizontal toward the N, 353°

Figure 5: Anisotropy map of two locations on OU2 tower for S post office winds and table of directions for average eigenvectors.

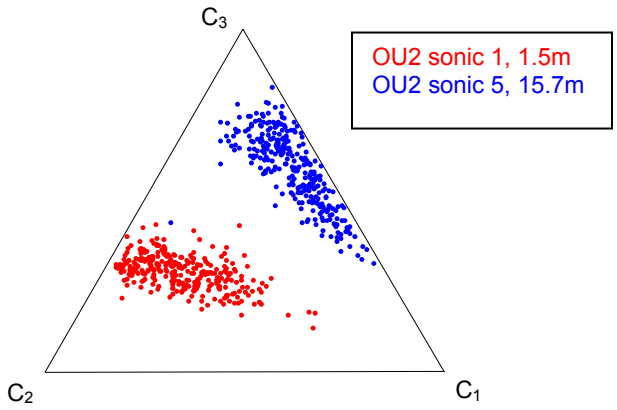

SW PO winds	Eigen vector	Average Direction of Eigenvector
1.5m	Λ_S (small)	5° from vertical toward the E, 75°
	Λ_B (large)	0.5° above horizontal toward the N, 358°
15.7m	Λ_S	42° from vertical toward the NE, 56°
	Λ_B	7.6° below horizontal toward the NNW, 343°

Figure 6: Anisotropy map of two locations on OU2 tower for SW post office winds and table of directions for average eigenvectors.

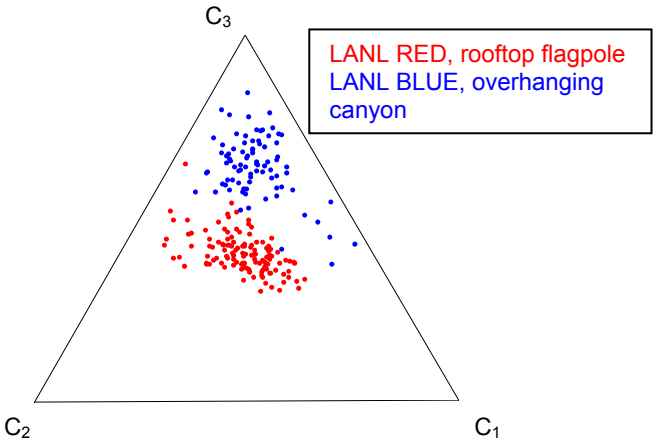

SE PO winds	Eigen vector	Average Direction of Eigenvector
roof	Λ_S (small)	14° from vertical toward the NNE, 68°
	Λ_B (large)	6.5° above horizontal toward the NW, 306°
Over hang	Λ_S	50° from vertical toward the NE, 56°
	Λ_B	35° below horizontal toward the NE, 50°

Figure 7: Anisotropy map of two locations on rooftops for SE post office winds and table of directions for average eigenvectors.

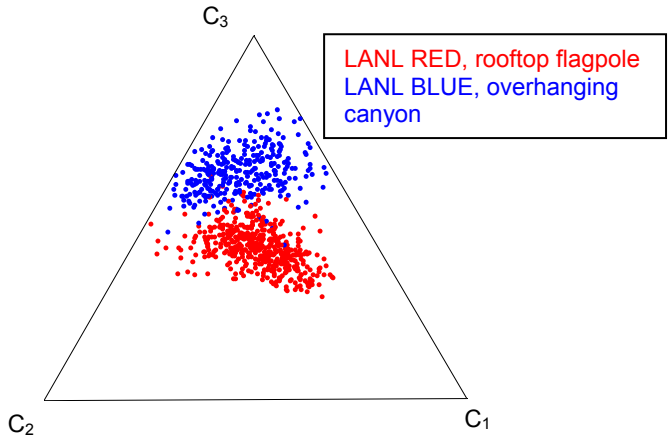

S PO winds	Eigen vector	Average Direction of Eigenvector
roof	Λ_S (small)	11° from vertical toward the E, 99°
	Λ_B (large)	8° above horizontal toward the WNW, 296°
Over hang	Λ_S	66° from vertical toward the NE, 32°
	Λ_B	43° below horizontal toward the N, 348°

Figure 8: Anisotropy map of two locations on rooftops for S post office winds and table of directions for average eigenvectors.

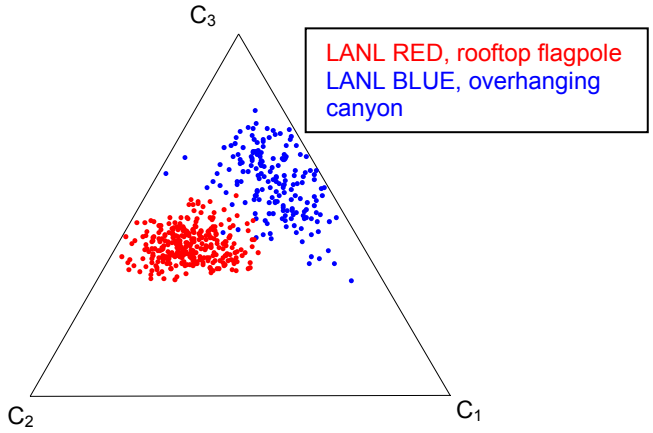

SW PO winds	Eigen vector	Average Direction of Eigenvector
roof	Λ_S (small)	8° from vertical toward the SE, 130°
	Λ_B (large)	4° above horizontal toward the NW, 306°
Over hang	Λ_S	69° from vertical toward the NE, 59°
	Λ_B	35° below horizontal toward the N, 357°

Figure 9: Anisotropy map of two locations on rooftops for SW post office winds and table of directions for average eigenvectors.

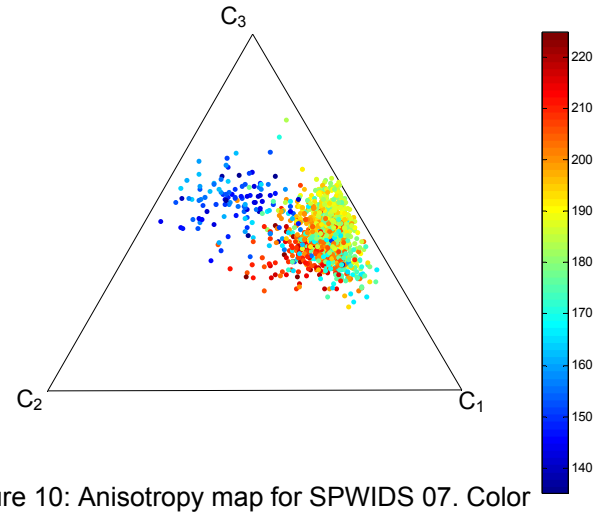

Figure 10: Anisotropy map for SPWIDS 07. Color indicates post office wind direction.

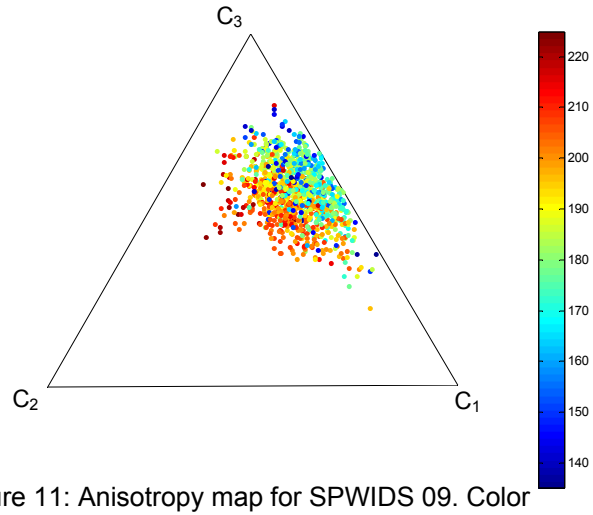

Figure 11: Anisotropy map for SPWIDS 09. Color indicates post office wind direction.

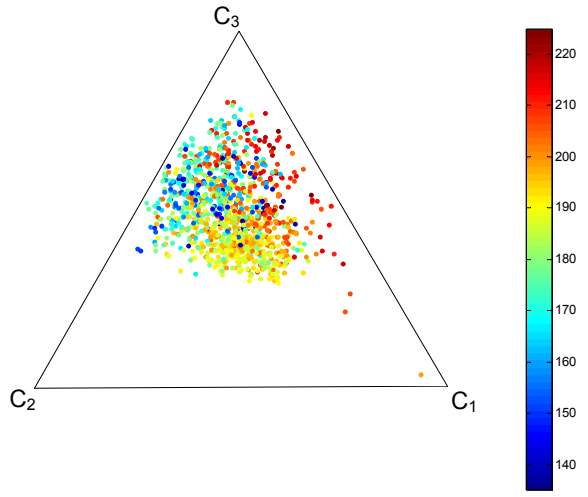

Figure 12: Anisotropy map for SPWIDS 12. Color indicates post office wind direction.

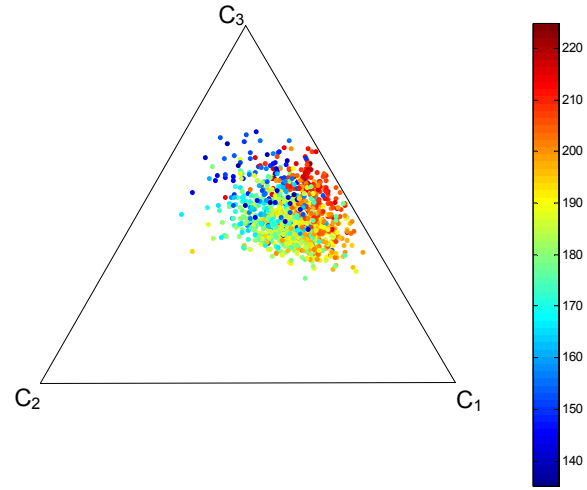

Figure 13: Anisotropy map for SPWIDS 14. Color indicates post office wind direction.